Evolution of metallic states from the Hubbard band in the two-dimensional Mott system BaCo$_{1-x}$Ni$_x$S$_2$

T. Sato,[1] H. Kumigashira,[1] D. Ionel,[1] T. Takahashi,[1] I. Hase,[2] H. Ding,[3] J. C. Campuzano,[4,5] and S. Shamoto[6]

[1]*Department of Physics, Tohoku University, Sendai 980-8578, Japan*
[2]*Electrotechnical Laboratory, Tsukuba 305-8568, Japan*
[3]*Department of Physics, Boston College, Chestnut Hill, Massachusetts 02467*
[4]*Department of Physics, University of Illinois at Chicago, Chicago, Illinois 60607*
[5]*Materials Sciences Division, Argonne National Laboratory, Argonne, Illinois 60439*
[6]*Department of Applied Physics, Tohoku University, Sendai 980-8579, Japan*

We report angle-resolved photoemission spectroscopy on the layered Mott system BaCo$_{1-x}$Ni$_x$S$_2$. (x =0.18, 0.28) across the phase transition from the antiferromagnetic insulator to anomalous metal. We found that the lower Hubbard band in the insulating phase possesses a remnant of the Fermi surface in the metallic phase and gradually evolves into the metallic bands with carrier doping. We compare the experimental result with those of the high-T_c cuprates to discuss the absence of superconductivity in BaCo$_{1-x}$Ni$_x$S$_2$.

Metal-insulator transition (MIT) has been one of the central subjects in solid state physics because it involves various essential physical concepts such as the strong correlation and charge order. In particular, MIT in a variety of Mott systems, where the electron correlation plays an important role, has been intensively studied theoretically and experimentally.[1] Photoemission spectroscopy has revealed several key features in the electronic structure which controls MIT, such as the coherent and incoherent parts at/near the Fermi level (E_F). Evolution of the electronic structure near E_F upon MIT has been studied by angle-resolved photoemission spectroscopy (ARPES) on insulating compounds.[2–4]

In this paper, we report ARPES study on BaCo$_{1-x}$Ni$_x$S$_2$ which is regarded as a layered Mott system like the cuprate high-temperature (high-T_c) superconductors. BaCo$_{1-x}$Ni$_x$S$_2$ has edge-sharing Co$_{1-x}$Ni$_x$S planes in the crystal-like CuO$_2$ planes in high-T_c superconductors and shows MIT from the antiferromagnetic insulator to the paramagnetic metal via the "anomalous" metallic phase upon Ni substitution.[5–10] The electrical and magnetic properties in the anomalous metallic phase look very similar to those of the high-T_c superconductors at the normal state,[6,7] but the superconductivity has not been observed down to 0.25 K.[11] It is thus very important to study the evolution of electronic structure near E_F across MIT in BaCo$_{1-x}$Ni$_x$S$_2$ and compare the result with high-T_c cuprates for understanding not only the mechanism of MIT but also the origin (or absence) of superconductivity in the high-T_c cuprates (BaCo$_{1-x}$Ni$_x$S$_2$).

Single crystals of BaCo$_{1-x}$Ni$_x$S$_2$ (x=0.18, 0.28) were grown by the self-flux method.[12] ARPES measurements were performed with a VSW HAC50 spectrometer at the undulator PGM beam line in SRC at Wisconsin. The energy and angular resolutions were set at 35 meV and $\pm1°$, respectively. We cleaved single crystals *in situ* to obtain a clean surface under vacuum of 5×10^{-11} Torr. Measurements were performed at 30 K within 12 hours after cleaving and during this time interval we did not observe degradation of sample surface. The Fermi level of sample was referenced to a gold

film, evaporated on the sample substrate and the accuracy is estimated to be better than 1 meV.

Figure 1 shows ARPES spectra near E_F for (a) metallic BaCo$_{0.72}$Ni$_{0.28}$S$_2$ and (b) insulating BaCo$_{0.82}$Ni$_{0.18}$S$_2$, measured with 40 eV photons along three different directions in the Brillouin zone (BZ). The electronic states in this energy range are ascribed to mainly the Co (Ni) 3d states.[13–15] We find that both sets of ARPES spectra look similar to each other, showing two main structures at 0.3 and 0.8 eV, respectively. In the metallic phase however, we clearly find an additional band which crosses E_F in the two directions [$X(R)$-$M(A)$ and $\Gamma(Z)$-$M(A)$], suggesting an electron-like Fermi surface (FS) centered at $M(A)$ point. In the insulating phase, on the other hand, the density of states (DOS) near E_F is remarkably suppressed and no clear E_F-crossing is seen in all directions, indicating an opening of a finite energy gap in the insulating phase.

Figure 2 shows the contour map of ARPES intensity at E_F obtained with the data within one octant of the BZ and consequent interpolation and symmetrization. The calculated FS's at $k_Z=0$ and π (Ref. 16) are shown for comparison. We find that the gross feature of FS shows a fairly good agreement between the experiment and the calculation; (1) the shape and volume of main large electron-like FS centered at $M(A)$ point and (2) a relatively weak intensity at the midpoint between $\Gamma(Z)$ and $M(A)$. In fact, the volume of main electron-like FS estimated from ARPES is $27\pm3\%$ of the whole BZ volume, in fairly good agreement with the electron count expected from the composition ($x=0.28$). In contrast, the present ARPES cannot clearly resolve the small FS's at $\Gamma(Z)$ or $X(R)$ predicted from the band calculation. This discrepancy may be due to the finite momentum resolution in the present ARPES and/or the three-dimensional nature of the FS's.

In order to study the evolution of electronic structure across MIT, we show the ARPES intensity as a function of momentum and binding energy (namely, band structure) for both compounds in Fig. 3, together with the second deriva-
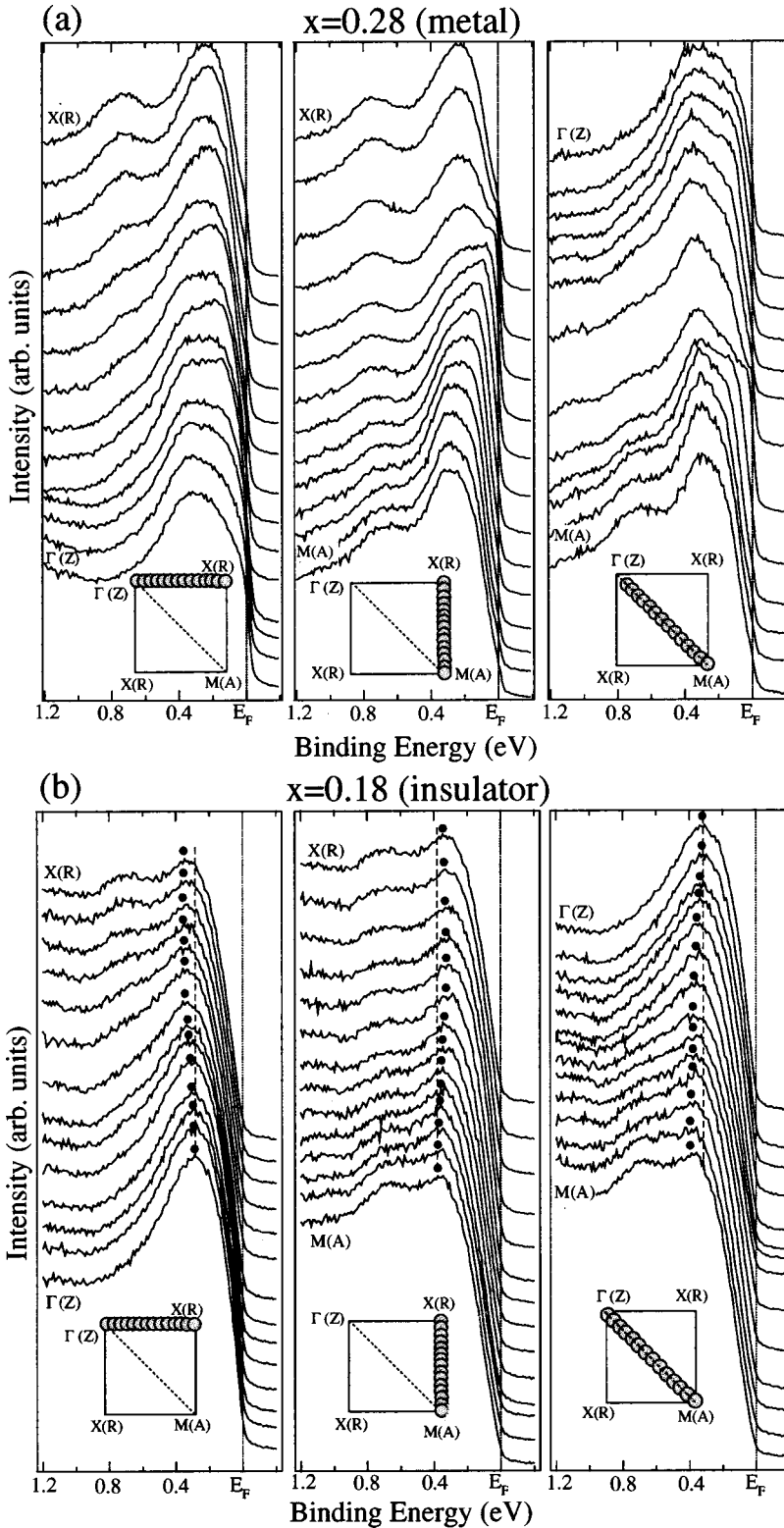
FIG. 1. ARPES spectra near E_F along $\Gamma(Z)-X(R)$, $X(R)-M(A)$ and $\Gamma(Z)-M(A)$ directions of $BaCo_{1-x}Ni_xS_2$ at (a) $x=0.28$ and (b) $x=0.18$, measured with 40-eV photons at 30 K. Corresponding k points are shown in the inset. Intensity of spectra is normalized with photon flux. Closed circle represents the position of peak maximum obtained from fitting around the peak top by Lorentzian. Straight dashed lines are guides for the eyes.

tive intensity to see small structures. The band structure calculation for $BaCo_{0.72}Ni_{0.28}S_2$ is also shown for comparison. In the experimental result for the metallic phase, we clearly find a dispersive band which crosses E_F in the two directions $M(A)$-$X(R)$ and $M(A)$-$\Gamma(Z)$. This band has the bottom around 0.2–0.3 eV at $M(A)$ point, forming a large electron-like FS centered at $M(A)$. We find that this experimental band is qualitatively well reproduced in the calculation. In order to determine the orbital character, we have performed a polarization-dependent measurement and found that when the polarization vector of photons is set within the mirror plane, the ARPES intensity near E_F is enhanced around $X(R)$ point [namely $(\pi, 0)$ point] while it is remarkably suppressed near $X'(R')$ point [$(0, \pi)$ point] (spectra not shown).
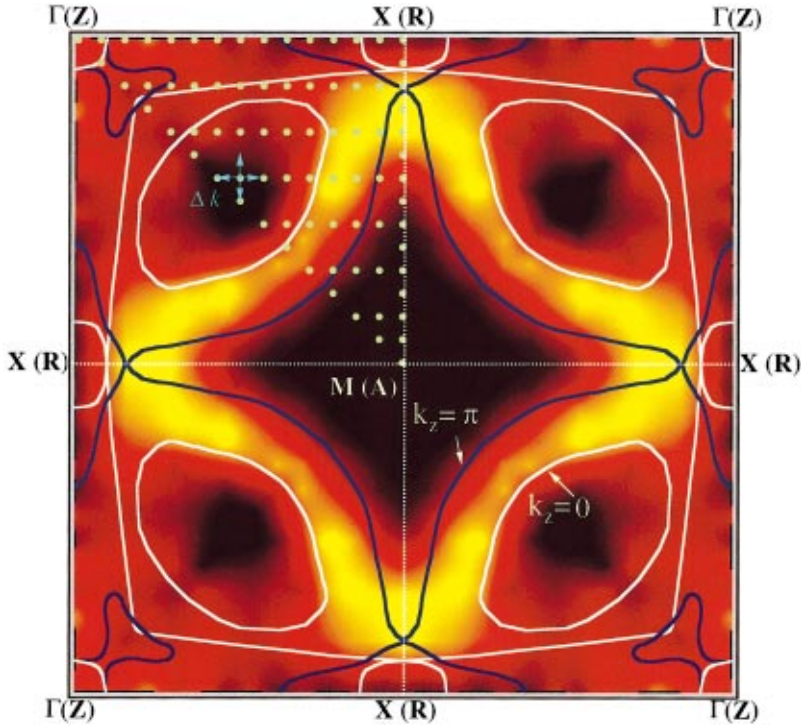
FIG. 2. (Color) Contour plot of ARPES spectral intensity at E_F (integrated from 2 meV below E_F to 2 meV above E_F) of metallic $BaCo_{0.72}Ni_{0.28}S_2$. Data taken at one octant of the Brillouin zone (white circles) are symmetrized and then interpolated. Corresponding k-resolution is shown by arrows. Bright areas represent the high intensity. Fermi surfaces cut at $k_Z=0$ and π are superimposed for comparison.

This indicates that the electronic states near E_F have an even symmetry with respect to the mirror plane.[17] This result is consistent with the band structure calculation which predicts a strong Co(Ni) $3d_{3z^2-r^2}$ character for the states near E_F, while the other even symmetry orbital, such as $d_{x^2-y^2}$, is not excluded experimentally. In Figs. 3(b) and 3(d), we find another dispersive band approaching E_F near $\Gamma(Z)$ point in the experimental band structure. Although it is not experimentally clear whether this band crosses E_F or not, it may correspond to a bunch of calculated bands which form small holelike FS's centered at $\Gamma(Z)$. Thus the present experimental result suggests that the doped electrons form mainly a large electronlike FS at $M(A)$ point and play an essential role in characterizing the transport and thermodynamic properties. This is consistent with the observed negative value of Hall coefficient and thermoelectric power.[7]

In the insulating phase, on the other hand, we find no clear E_F crossing of band [Figs. 3(a) and 3(c)]. We have performed additional ARPES measurements for several cuts within one octant of the BZ (see Fig. 2) and confirmed no E_F crossing. This is consistent with the insulating nature of $BaCo_{0.82}Ni_{0.18}S_2$, suggesting that a Mott-Hubbard gap opens in the insulating phase and the broad band at 0.2–0.3 eV is assigned as a lower Hubbard band. We find in Figs. 3(c) and 3(d) that a weak structure at 0.6–0.8 eV is slightly shifted toward high-binding energy by a few tens meV from $x = 0.18$ to 0.28. This is explained in terms of the chemical-potential shift caused by the electron doping, consistent with the estimation from the band calculation (30 meV from $x = 0.2$ to 0.3).[15] In contrast, the band dispersion near E_F clearly deviates from this simple rigid-band picture; the experimental band near E_F approaches E_F with doping. This is obviously against the prediction from the band calculation, indicating importance of the electron correlation for under-

standing the MIT. The most drastic change across MIT is the appearance of dispersive bands near E_F in the metallic phase. One of the most essential questions for understanding MIT is where and how these dispersive metallic bands are created. In Figs. 3(a) and 3(c), we clearly find "wiggling" of band in the almost "flat" lower Hubbard band in the insulating phase. Further, the maximal position of bands in the insulating phase (indicated by arrows) almost coincide with the E_F crossing point of the dispersive band in the metallic phase. This suggests that the band dispersion in the insulating phase has a remnant nature of the metallic dispersion. Figure 4 shows the momentum distribution function $n(k)$ for both the insulating and metallic phase, obtained by integrating ARPES intensity from 200 meV below E_F to 100 meV above E_F. Although the change of $n(k)$ as a function of momentum is small in the insulating phase, the $n(k)$'s of both phases share some common features, such as the high intensity midway between $X(R)$ and $M(A)$ points as well as around $\Gamma(Z)$ and a relatively weak intensity midway between $\Gamma(Z)$ and $M(A)$. These experimental results suggest that the lower Hubbard band inherently possesses a "remnant Fermi surface" away from E_F in the insulating phase and the metallic dispersive band forming a "real Fermi surface" born from the lower Hubbard band. In other words, the lower Hubbard band gradually evolves into the metallic band.

Next, we discuss the origin for the insulating nature of $BaCo_{1-x}Ni_xS_2$ at $x=0.18$. The structural distortion observed in $BaCoS_2$[6] seems unlikely since the lattice instability due to the monoclinic distortion is quickly suppressed with Ni substitution and is no longer present at $x>0.1$.[6] If the antiferromagnetic ordering plays a key role, a band-folding associated with the magnetic-ordering vector[8] is expected to be observed. However, the ARPES result does not show any indi-
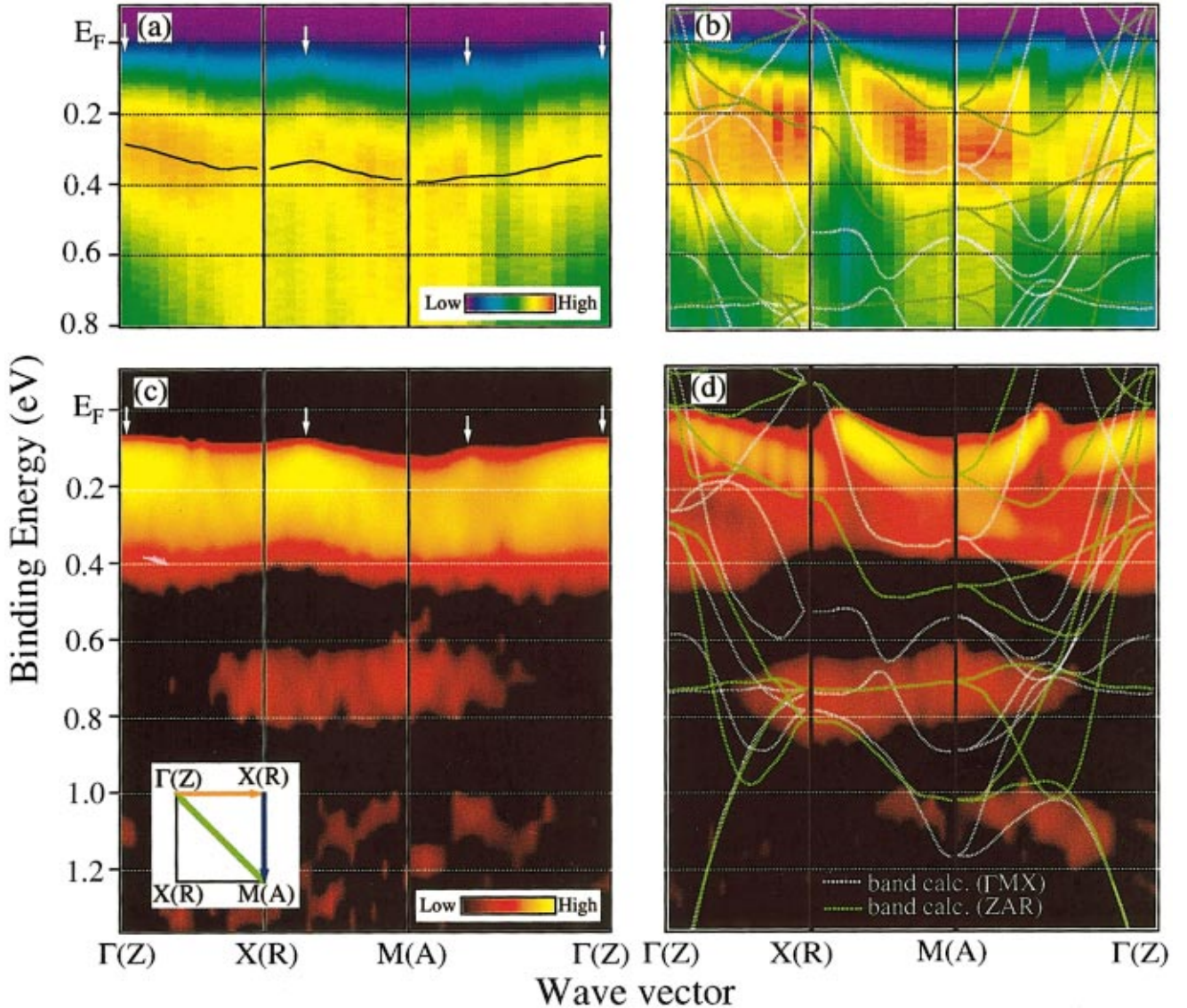
FIG. 3. (Color) Comparison of band structures between insulating $BaCo_{0.82}Ni_{0.18}S_2$ and metallic $BaCo_{0.72}Ni_{0.28}S_2$ derived from the ARPES intensity plot [(a), (b)] and the second derivative image [(c), (d)]. Band structure calculation of $BaCo_{0.72}Ni_{0.28}S_2$ on high-symmetry lines is superimposed for comparison. Black solid line in (a) traces the peak position. Maximal points of band in the insulating phase are indicated by arrows.

cation of the band-folding, which may be related to the weak exchange coupling $J = 7-8$ meV reported recently by Raman scattering.[18] Further, the energy scale dominating the MIT (order of 0.1 eV as found in Fig. 3) seems much larger than J in contrast with the case of the high-T_c cuprate $(Sr_2CuO_2Cl_2)^2$, where the observed band width (~ 0.3 eV) is comparable to the exchange energy ($2.2J$), but far smaller than the prediction from the band calculation. This suggests that the antiferromagnetism plays a less important role for the phase transition in $BaCo_{1-x}Ni_xS_2$ than in high-T_c cuprates. On the other hand, considering the relatively narrow band width near E_F in $BaCo_{0.82}Ni_{0.18}S_2$ compared with the band calculation, it is inferred that the electron correlation among d electrons has still an essential role in characterizing the insulating nature at $x = 0.18$, and the MIT may be understood in terms of the successive change in the effective cor-

relation energy with Ni substitution.

Finally we briefly comment on the electronic structure of the anomalous metallic phase ($x = 0.28$) in relation to the high-T_c cuprates. We find no obvious nesting vectors in the FS (Fig. 2), consistent with the fact that no charge ordering has been observed in $BaCo_{1-x}Ni_xS_2$ ($x = 0.28$). We also find no indication for the band-folding (so-called a shadow band) due to the local antiferromagnetic ordering in contrast with the high-T_c cuprates.[19] This is consistent with disappearance of the antiferromagnetic ordering in the anomalous metallic phase.[7] Further, we do not observe a flat band close to E_F at the zone boundary, known as van-Hove singularity (VHS) commonly seen in the hole-doped high-T_c cuprates.[20] Suppose that VHS is a necessary condition for the high-T_c superconductivity, the present result may explain the absence of superconductivity in $BaCo_{1-x}Ni_xS_2$. It is also remarked

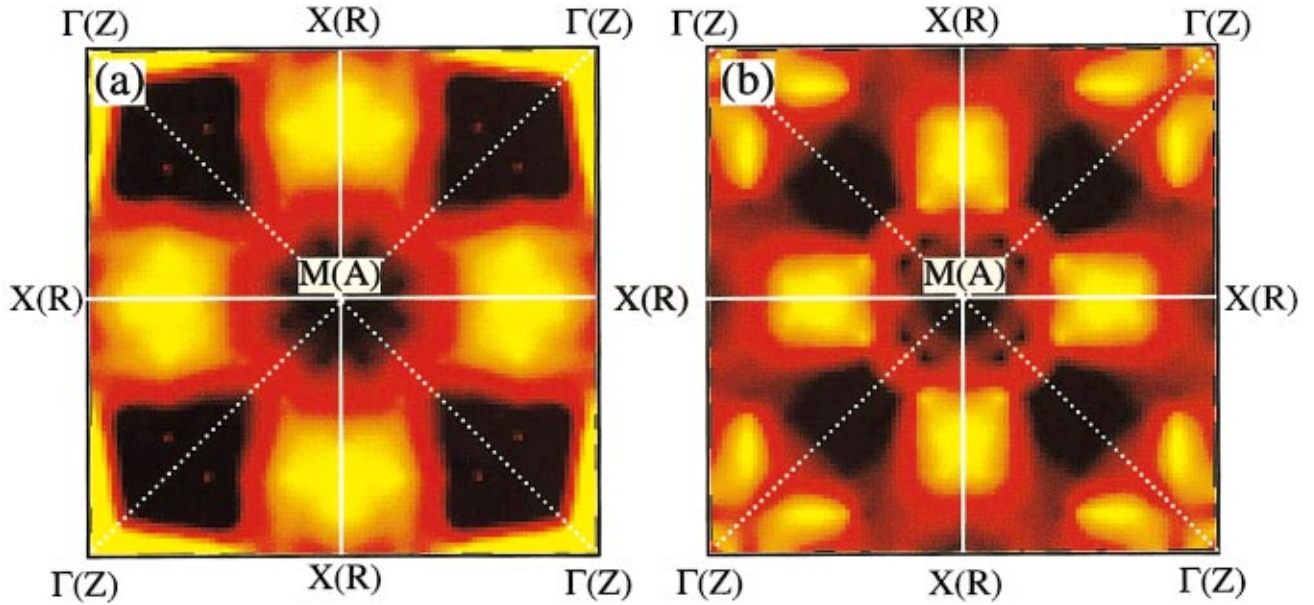FIG. 4. (Color) Comparison of momentum distribution function $n(k)$ between (a) insulating $BaCo_{0.82}Ni_{0.18}S_2$ and (b) metallic $BaCo_{0.72}Ni_{0.28}S_2$. To obtain $n(k)$, ARPES intensity is integrated from 200 meV below E_F to 100 meV above E_F. Intensity higher than 80% of the maximum intensity is shown for better comparison. Symmetrization and interpolation are used as in Fig. 2.

that the electronic states responsible for the thermodynamic properties originate predominantly in the Co(Ni) $3d_{z^2-r^2}$ orbital which stands perpendicular to the $Co_{1-x}Ni_xS$ plane in $BaCo_{1-x}Ni_xS_2$, while those in the high-T_c cuprates are from the Cu $3d_{x^2-y^2}$ orbital lying within the CuO_2 plane. All these facts suggest that the electronic structure of $BaCo_{1-x}Ni_xS_2$ is basically different from that of the high-T_c cuprates, although the transport and magnetic properties share some common features between the two layered compounds.[6,7]

In conclusion, we have performed high-resolution angle-resolved photoemission spectroscopy on $BaCo_{1-x}Ni_xS_2$ to study the electronic structure and its evolution across the MIT. The experimental result shows that the strong electron correlation plays an essential role in characterizing the electronic structure and its evolution. We found that the lower

Hubbard band in the insulating phase possesses a remnant of the Fermi surface in the metallic phase and gradually evolves into the metallic bands with carrier doping, like in the high-T_c cuprates. On the other hand, we found some different features in the electronic structure, such as the dominant $3d_{3z^2-r^2}$ nature of the E_F crossing band, the absence of van-Hove singularity, and the relatively small exchange energy J compared with the energy scale near E_F. All these clearly differentiate $BaCo_{1-x}Ni_xS_2$ from the high-T_c cuprates.

[1] M. Imada, A. Fujimori, and Y. Tokura, Rev. Mod. Phys. **70**, 1039 (1998).

[2] B. O. Wells, Z.-X. Shen, A. Matsuura, D. M. King, M. A. Kastner, M. Greven, and R. J. Birgeneau, Phys. Rev. Lett. **74**, 964 (1995).

[3] F. Ronning, C. Kim, D. L. Feng, D. S. Marshall, A. G. Loeser, L. L. Miller, J. N. Eckstein, I. Bozovi, and Z.-X. Shen, Science **282**, 2067 (1998).

[4] S. Haffner, C. G. Olson, L. L. Miller, and D. W. Lynch, Phys. Rev. B **61**, 14 378 (2000).

[5] I. E. Grey and H. Steinfink, J. Am. Chem. Soc. **92**, 5093 (1970).

[6] L. S. Martinson, J. W. Schweitzer, and N. C. Baenziger, Phys. Rev. Lett. **71**, 125 (1993); Phys. Rev. B **54**, 11 265 (1993).

[7] J. Takeda, K. Kodama, H. Harashina, and M. Sato, J. Phys. Soc. Jpn. **63**, 3564 (1994); J. Phys. Soc. Jpn. **64**, 2550 (1995).

[8] K. Kodama, S. Shamoto, H. Harashina, J. Takeda, M. Sato, K. Kakurai, and M. Nishi, J. Phys. Soc. Jpn. **65**, 1782 (1996).

[9] S. Shamoto, K. Kodama, H. Harashina, M. Sato, and K. Kakurai, J. Phys. Soc. Jpn. **66**, 1138 (1997).

[10] Y. Yasui, H. Sasaki, S. Shamoto, and M. Sato, J. Phys. Soc. Jpn. **66**, 3194 (1997).

[11] Y. Yasui (private communication).

[12] S. Shamoto, S. Tanaka, E. Ueda, and M. Sato, Physica C **263**, 550 (1996); J. Cryst. Growth **154**, 197 (1995).

[13] We have checked photon-energy dependence of normal emission spectra from 22 eV up to 42 eV where states within 1 eV from E_F were strongly enhanced as higher photon energies. Band-structure calculation also predict d-derived states near E_F (Refs. 14 and 15).

[14] L. F. Mattheiss, Solid State Commun. **93**, 879 (1995).

[15] I. Hase, N. Shirakawa, and Y. Nishihara, J. Phys. Soc. Jpn. **64**, 2533 (1995).

[16] Band structure calculation is performed by using the scalar-relativistic full-potential linearized augmented plane wave (FLAPW) method within the local-density approximation (LDA). Details of the calculation have been described elsewhere (Ref. 15).

[17] For example, see Hüfner, *Photoelectron Spectroscopy* (Springer-Verlag, Berlin, 1994).

[18] K. Takenaka, S. Kashima, A. Osuka, S. Sugai, Y. Yasui, S. Shamoto, and M. Sato, Phys. Rev. B **63**, 115113 (2001).

[19] P. Aebi, J. Osterwalder, P. Schwaller, L. Schlapbach, M. Shimoda, T. Mochiku, and K. Kadowaki, Phys. Rev. Lett. **72**, 2757 (1994).

[20] K. Gofron, J. C. Campuzano, A. A. Abrikosov, M. Lindroos, A. Bansil, H. Ding, D. Koelling, and B. Dabrowski, Phys. Rev. Lett. **73**, 3302 (1994).